

Electronic supplementary information for Polysulfone-nanodiamond composite membranes: A novel gamma radiation resistant material

*Amita Bedar,^{a,b} Nitesh Goswami,^b Amit K. Singha,^b Virendra Kumar,^c Anil K. Debnath,^d
Debasis Sen,^{a,e} Vinod K. Aswal,^{a,e} Sanjay Kumar,^f Dhanadeep Dutta,^g Biju
Keshavkumar,^h Sharwari Ghodke,ⁱ Ratnesh Jain,ⁱ Beena G. Singh,^{a,j} Pradeep K.
Tewari,^a Ramesh C. Bindal,^{a,b} and Soumitra Kar,^{*a,b}*

^a Homi Bhabha National Institute, Mumbai–400094, India. E-mail: soubiswa@barc.gov.in, soumitra.1stmay@gmail.com

^b Membrane Development Section, Bhabha Atomic Research Centre, Trombay, Mumbai – 400085, India

^c Radiation Technology Development Division, Bhabha Atomic Research Centre, Trombay, Mumbai – 400085, India

^d Technical Physics Division, Bhabha Atomic Research Centre, Trombay, Mumbai – 400085, India

^e Solid State Physics Division, Bhabha Atomic Research Centre, Trombay, Mumbai – 400085, India

^f Material Science Division, Bhabha Atomic Research Centre, Trombay, Mumbai – 400085, India

^g Radiochemistry Division, Bhabha Atomic Research Centre, Trombay, Mumbai – 400085, India

^h Health Physics Division, Bhabha Atomic Research Centre, Trombay, Mumbai – 400085, India

ⁱ Department of Chemical Engineering, Institute of Chemical Technology, Mumbai– 400019, India

^j Radiation & Photochemistry Division, Bhabha Atomic Research Centre, Trombay, Mumbai – 400085, India

S1. Attenuated total reflectance Fourier-transform infrared spectroscopy (ATR-FTIR) of the membranes

Figure S- I shows the FTIR spectra of 500 kGy irradiated membranes. Absence of any additional peak in the FTIR spectra (compared to their unirradiated counter parts) confirms no distinct functional group is formed with irradiation.

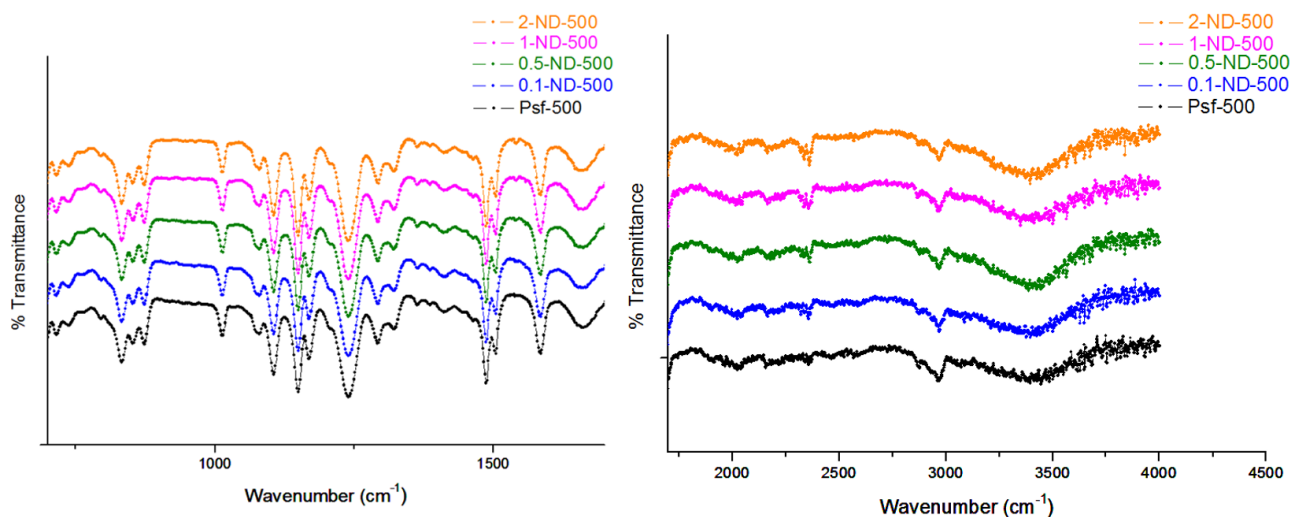


Figure S- I: ATR-FTIR analysis of the control Psf and Psf-ND composite membranes, all 500 kGy irradiated membranes.

S2. X-ray photoelectron spectroscopy (XPS) of the membranes

Figure S- II shows the XPS spectra for S-2p peak of unirradiated membranes. XPS spectra exhibits binding energy peak for S-2p_{3/2} bond around 168 eV, and S-2p_{1/2} bond around 169.2 eV. Figure S- III shows the XPS spectra for O-1s peak of unirradiated membranes. XPS spectra exhibits binding energy peak for O bond from sulfate around 531.1 eV, S=O bond around 532.2 eV, and S-OH bond around 533.2 eV. No shift in the XPS peaks of the bonds confirms

that there is no chemical interaction between the ND and Psf, even at increased loading of ND, indicating only physical entrapment of nanomaterials in the membrane matrix.

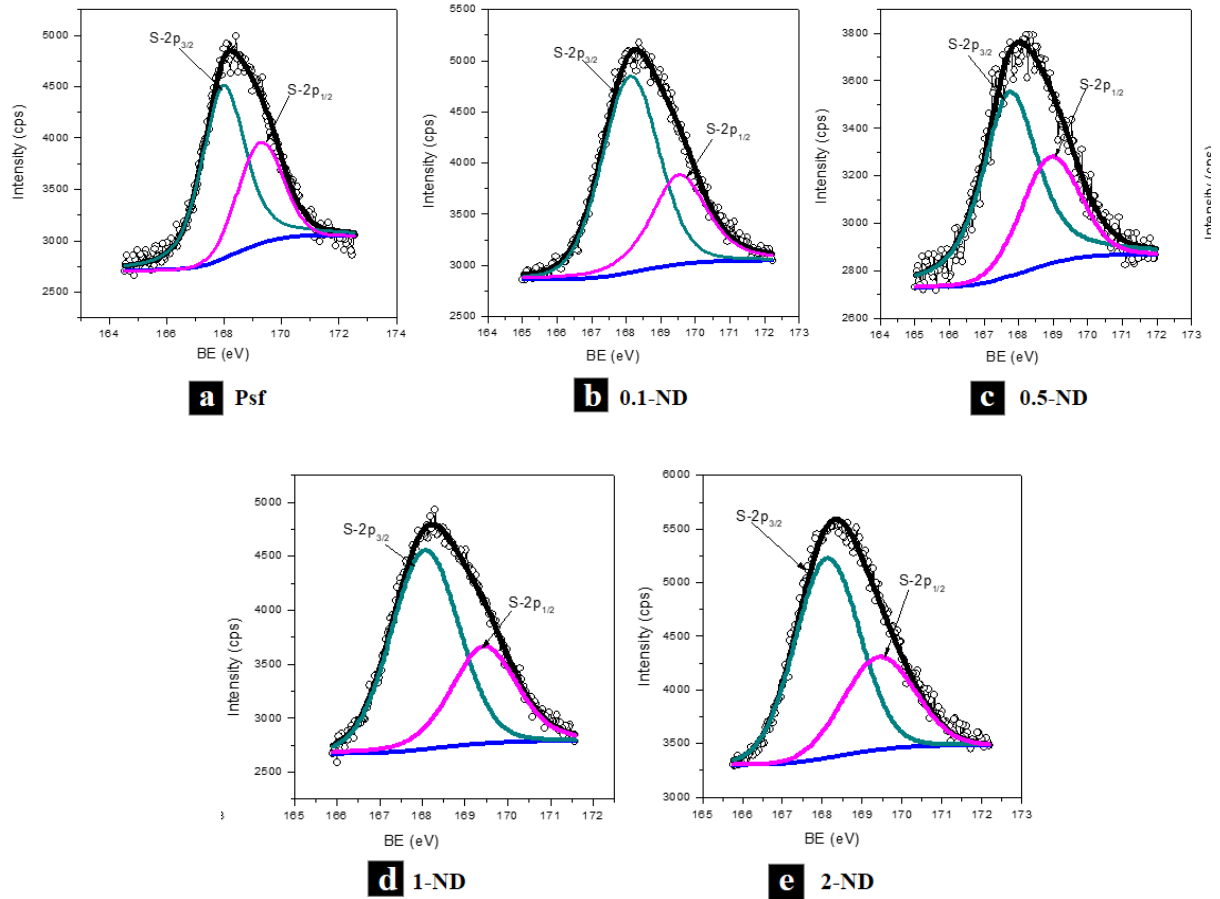


Figure S- II: X-ray photoelectron spectra (XPS) of S-2p peak of the membranes: (a) Psf, (b) 0.1-ND, (c) 0.5-ND, (d) 1-ND, and (e) 2-ND.

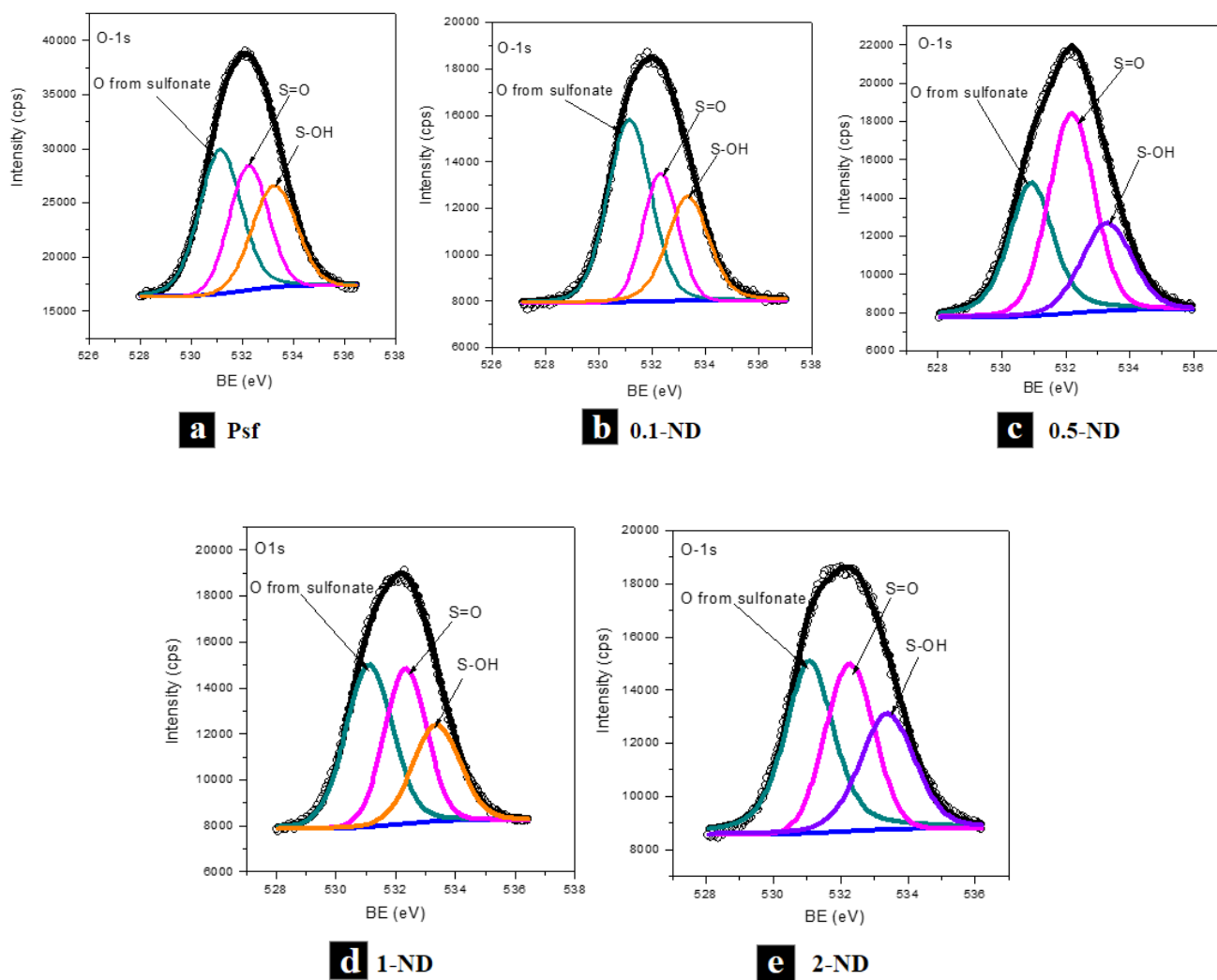


Figure S- III: X-ray photoelectron spectra (XPS) of O-1s peak of the membranes: (a) Psf, (b) 0.1-ND, (c) 0.5-ND, (d) 1-ND, and (e) 2-ND.

Figure S- IV shows the XPS spectra for C-1s peak of 1000 kGy irradiated membranes. XPS spectra exhibits binding energy peak for C-C bond around 284.9 eV, C-OH bond around 286.3 eV, and C=O bond around 287.5 eV. Absence of additional peaks in the membrane samples exposed to gamma irradiation (compare to unirradiated membrane) confirms no adduct formation with irradiation.

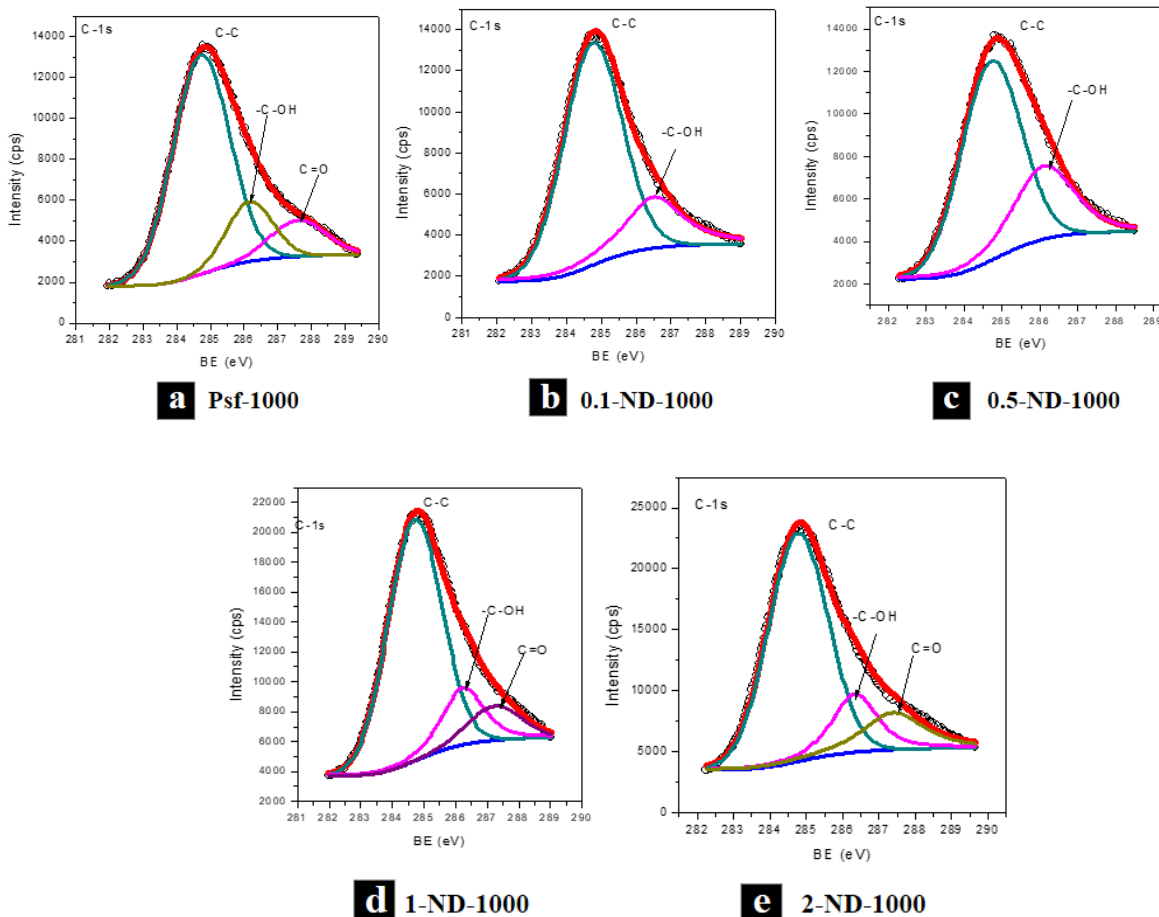


Figure S- IV: X-ray photoelectron spectra (XPS) of C-1s peak of the membranes: (a) Psf-1000, (b) 0.1-ND-1000, (c) 0.5-ND-1000, (d) 1-ND-1000, and (e) 2-ND-1000.

S3. Small angle X-ray scattering (SAXS) curve of the membrane

SAXS experiments were performed using a laboratory-based SAXS instrument with Cu K_{α} ($\lambda=1.54 \text{ \AA}$) as probing radiation. Radial averaged scattering intensity ($I(q)$) was done within a wave vector transfer ($q = 4\pi \sin(\theta)/\lambda$, where λ is the wavelength and 2θ is the scattering angle) range from ~ 0.1 to 2.5 nm^{-1} . The sample to detector distance was nearly 1 m.

Figure S- V shows the scattering curve of the membrane with different composition and at different radiation dose. By fitting the curve, it was found that three cumulative power law

scattering contribution could explain fairly well the scattering profile of the Psf membrane. C_n is q independent constant parameter (proportional to the product of number density of the particle and the respective scattering contrast) for membrane, and was estimated by fitting model to the scattering curve of each membrane using non-linear least square method.

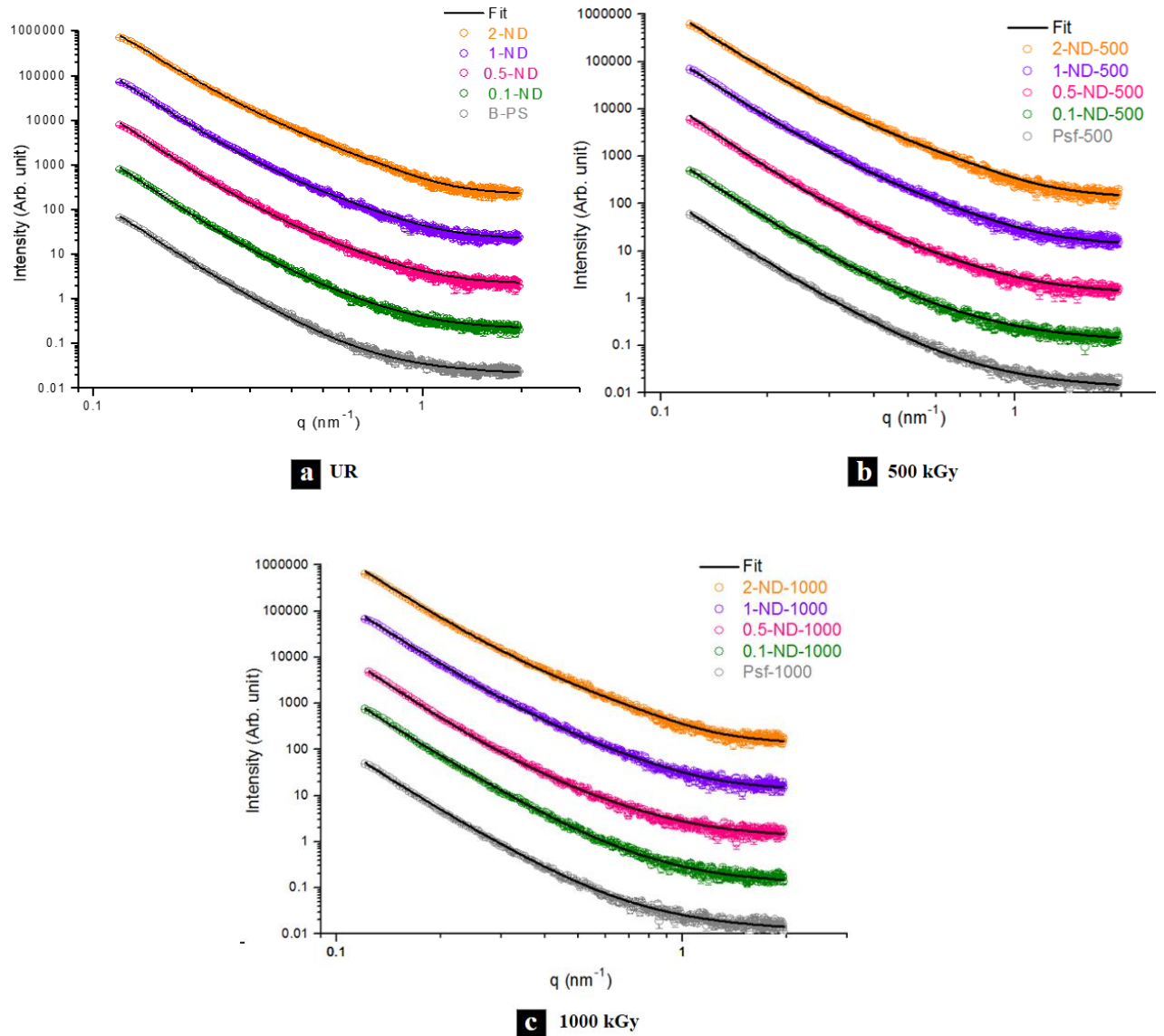


Figure S- V: Small angle X-ray scattering (SAXS) curve fitting for the membranes: (a) Unirradiated, (b) 500 kGy radiation dose, and (c) 1000 kGy radiation dose.

Figure S- VI shows the particle size distribution obtained from small angle X-ray scattering. Average diameter size of the ND particles acquire around 4.9 nm. This size distribution was used during the fitting of SAXS curve for Psf-ND composite membranes.

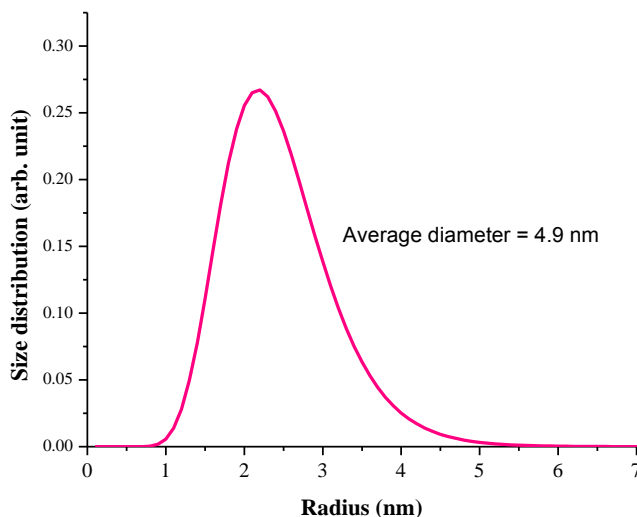
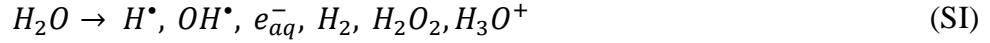


Figure S- VI: Particle size distribution of nanodiamond powder.

S4. Pulse radiolysis studies for evaluation of free radical scavenging capability of membranes

Pulse radiolysis experiments were carried out with high-energy electron pulses (7 MeV, 500 ns) obtained from a linear electron accelerator. The transient species formed on pulse radiolysis were detected by optical absorption method. Aerated aqueous solution of KSCN (1×10^{-2} M) was used for determining the dose delivered per pulse, monitoring the transient $(\text{SCN})_2^{\bullet-}$ at 475 nm, using $G\epsilon (475 \text{ nm}) = 2.59 \times 10^{-4} \text{ m}^2/\text{J}$. Here, G denotes the radiation chemical yield in mol/J and ϵ denotes the molar extinction coefficient in $\text{m}^2\text{mol}^{-1}$. The dose per pulse was close

to 10-12 Gy/ pulse (1 Gy = 1 J kg⁻¹). Radiolysis of N₂-saturated neutral aqueous solution leads to the radiolysis of water as given in equation SI.



In the present studies, the ability of the Psf-ND composite membranes to scavenge e_{aq}^- was investigated using membrane coupons of $3 \times 1 \text{ cm}^2$ immersed in DI water, and compared with the control Psf membrane. Among the radicals generated, the yield of the hydroxyl (OH[•]) and hydrated electron (e_{aq}^-) are relatively high at neutral pH. The OH[•] radicals and e_{aq}^- are strongly oxidizing and reducing in nature, respectively. Therefore, in order to investigate the reaction of the polymer composite with e_{aq}^- , 1 M tert-butanol was added to the aqueous solution to scavenge the OH[•] radicals, giving a total radiation chemical yield (G value) of 0.27 $\mu\text{mol/J}$ under N₂ saturated condition.

The characteristic absorption spectrum of e_{aq}^- has a broad, structureless band with a maximum around 700 nm in aqueous system. In general, the reactivity of the e_{aq}^- is investigated by monitoring the time absorption plot at 700 nm in presence of different concentration of solute. In the present studies, the ability of the Psf-ND composite membranes to scavenge e_{aq}^- was investigated and compared with the control Psf membrane (Figure S- VII). The absorbance of e_{aq}^- at 700 nm decayed by following first order kinetics with a rate of $2.0 \pm 0.5 \times 10^5 \text{ s}^{-1}$, which increased slightly in presence of control Psf membrane ($3.7 \pm 0.8 \times 10^5 \text{ s}^{-1}$). However, the rate of decay was found to increase with ND loading, with about 3 times enhancement for 2-ND composite membrane ($1.2 \pm 0.4 \times 10^6 \text{ s}^{-1}$), compared to that of control Psf. The scavenging of the e_{aq}^- radical by ND (nanomaterial alone) was confirmed by monitoring their reaction with varying concentration of ND particles (Figure S- VIII). The results showed that increasing ND

concentration leads to rapid decay of the hydrated electron, which confirms that ND is responsible for scavenging the radiolysed product (free radical) of water. Interestingly, this unique attribute of ND was translated to the composite membrane matrix and therefore, the latter was found to exhibit enhanced radiation resistance properties, compared to the control Psf membrane.

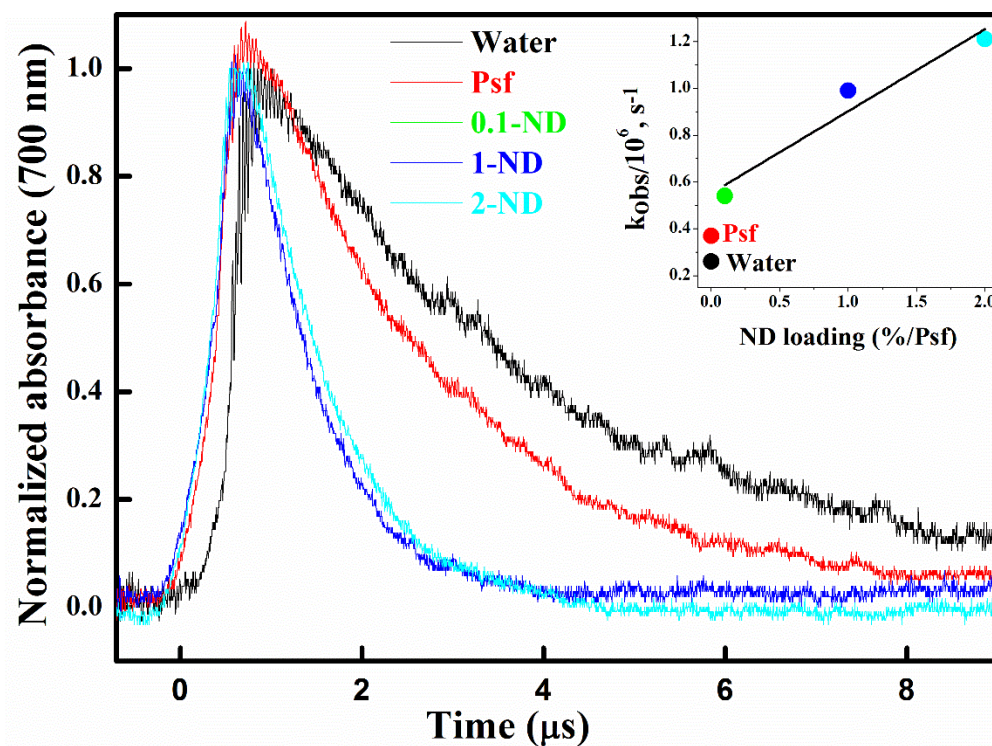


Figure S- VII: Absorption-time plot of hydrated electron of water at 700 nm in absence and presence of Psf-ND composite membrane with different loading of ND in the Psf matrix. Inset shows plot of observed rate as a function of Psf-ND composite membrane with different loading of ND at pH 7.

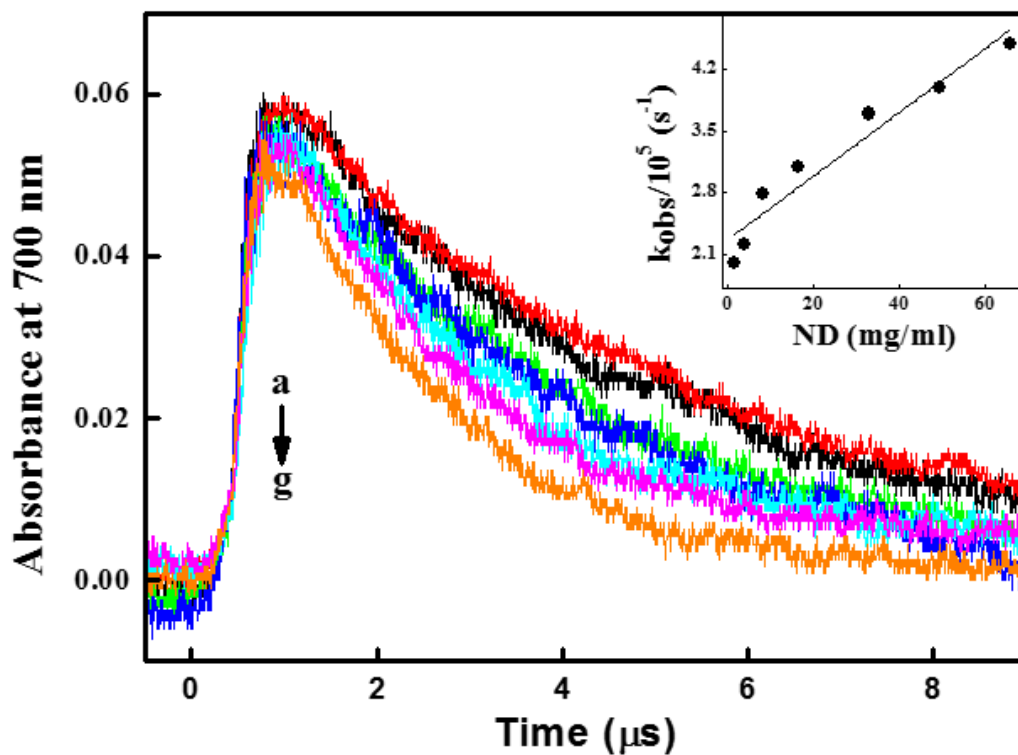


Figure S- VIII: Absorption-time plot of hydrated electron of water at 700 nm in presence of varying concentration of ND particles suspended in aqueous solution containing 1 M t-butanol at pH 7 under N_2 saturated condition. Here plot corresponds ND concentration at (a) = 1.65 $\mu\text{g/ml}$, (b) = 4.12 $\mu\text{g/ml}$, (c) = 8.25 $\mu\text{g/ml}$, (d) = 16.5 $\mu\text{g/ml}$, (e) = 33 $\mu\text{g/ml}$, (f) = 49.5 $\mu\text{g/ml}$, (g) = 66 $\mu\text{g/ml}$. Inset shows the plot of observed rate of hydrated electron as a function of ND particles concentration at pH 7.